LAUTECH Journal of Engineering and Technology 17 (1) 2023: 96-106

OPTIMAL PLACEMENT OF UNIFIED POWER FLOW CONTROLLER ON POWER SYSTEM FOR VOLTAGE STABILITY ENHANCEMENT USING ARTIFICIAL NEURAL NETWORK TECHNIQUE

[1]Fehintola, O. T; [1]Adejumobi, I. A; [1]Amusa, K. A and [2]Olajuwon, B. I.

[1]Department of Electrical/Electronics Engineering, Federal University of Agriculture, Abeokuta, Nigeria.
[2]Department of Mathematics, Federal University of Agriculture, Abeokuta, Nigeria.
Corresponding Author: engradejumobi@yahoo.com

ABSTRACT

The desire for an enhanced power transfer capability and quality of electricity delivered to the customers has led to emergence of Flexible Alternating Current Transmission Systems (FACTS). This work compares power system voltage stability with and without compensation. The compensation is done by optimal placement of Unified Power Flow Controller (UPFC) using Artificial Neural Network (ANN) technique. The algorithm to implement the stabilizing processes employed Newton-Raphson-based load flow equations in MATLAB R2018a environment. The stability of Nigerian 330 kV, 30–bus network was assessed before and after the implementation of UPFC and UPFC-ANN controlled. The results obtained without compensation showed: New Haven, Onitsha, Gombe, Jos, Kano and Calabar with voltage magnitude of 0.9003, 0.9468, 0.6608, 0.8141, 0.8138 and 0.9319 p.u, respectively violated the statutory limit of $0.95 \leq V_i \leq 1.05$ p.u and total active power loss was 218.76 MW. With UPFC on bus Calabar, the total active power loss reduced to 200.85 MW, while buses New Haven, Gombe, Jos and Kano produced voltage magnitude of 0.9130, 0.6608, 0.8141 and 0.8138 p.u, respectively, still constrained. ANN based UPFC placement on bus Gombe - the most critical bus with Voltage stability index (VSI) of 0.9252, the voltage magnitude of buses New Haven, Onitsha, Gombe, Jos, Kano and Calabar enhanced to 0.9533, 0.9552, 1.0481, 1.0399, 1.0425 and 1.0081 p.u, respectively and total active power loss reduced by 28.81% compared with 8.19% reduction with UPFC. The study revealed ANN controlled UPFC is suitable and appropriate for improving voltage stability and reducing power loss on power system.

Keywords: *Flexible Alternating Current Transmission Systems (FACTS); Artificial Neural Network (ANN); Voltage Stability Index (VSI); Unified Power Flow Controller (UPFC); voltage stability; active power loss; voltage magnitude.*

INTRODUCTION

One of the major challenges facing Power System Engineers during planning and operations of systems is voltage instability. For a normal operation, it is essential to maintain the required system voltage Profiles with stable and reliable power flow. Voltage instability is the cause of many serious system collapses during grid operations (Chappa and Thakur, 2020). According to Ezeruigbo *et al.* (2021), "voltage stability of a power system is its ability to maintain steady and acceptable voltages at all buses in the system under normal operating conditions and also after being subjected to a disturbance". Usually, voltage stability are ensured by the use of transformers, capacitor banks, reactors etc. However, these methods have not been effective because of their electro-mechanical nature, slow response times, high maintenance costs, lack of operational flexibility and versatility required for effective voltage stability control (Muhammad *et al.,* 2020).

The quest for a reliable, flexible and efficient electrical power systems, results into a high-power

electronics-based technology for transmission systems called Flexible Alternative Current Transmission Systems (FACTS) controllers. FACTS improves the stability and ensures the line loadings are closer to the thermal limits. The technology has more initial cost outlay as compared with the electro-mechanical ones with little or no maintenance cost (Gupta *et al.*, 2022). To derive maximum benefits from FACTS controllers, they must be optimally located on the line(s) with the right type and rating must be considered.

FACTS controllers are classified into four types as a result of connections to the lines namely; the shunt controllers, the series controllers, the combined series-shunt controllers and the combined series-series controllers (Patel *et al.,* 2014). For this study, a combined series-shunt controller named Unified Power Flow Controller (UPFC) was considered because it ranks highest in term of completeness among the controllers due to its ability and versatility to control the three line parameters; voltage, phase angle and impedance which determine the value of transmitted power (Noor *et al.*, 2013). Unified power flow controller is a fast acting and versatile FACTS controller. To make the placement of UPFC faster and accurate, an Artificial Intelligence (AI) technique is coupled to the unified power flow controller to resolve the aforementioned problem by issuing quick real time system control instructions to the controller (Mutegi *et al*., 2015). The family of Artificial intelligence technique employed in this work to optimally place the UPFC for power system voltage stability enhancement considering Nigerian 30-bus electricity grid as test case was Artificial Neural Networks (ANNs). The choice of ANN in this study was due to its ability to decipher and properly classify highly non-linear problems, ability for algorithms learning, an online adaption of dynamic systems, ability to carry out parallel computation quickly and intelligently interpolate data (Rajesh, 2018).

LITERATURE REVIEW

Many efforts have been put forward by power system researchers and engineers to investigate the effect of application of FACTS devices such as UPFC on the voltage stability of power system network. Idris and Abel (2021) focused on the use of unified power flow controller for voltage stability enhancement in an interconnected network. The work optimally located UPFC in the considered power system network. The effect of application of Generalized Unified Power Flow Controller (GUPFC) for voltage stability improvement in power system was examined by Alhassan *et al*. (2020). The study developed a multi-objective optimization function by minimizing active power loss and voltage variation in determining the optimal size and location of GUPFC with the use of Particle Swarm Optimization (PSO) approach. The results from the study showed a significant improvement in voltage profile and total active power loss.

Kumar (2019) proposed optimal location of UPFC using heuristic technique for power system performance improvement. For optimum location of UPFC on the Institute of Electrical and Electronics Engineers (IEEE) 30-bus power network considered as the case study, Artificial Bee Colony Algorithm (ABC) was employed and implemented in MATLAB environment. Results from the study revealed that voltage profile and power losses on the considered test network were significantly improved.

Binary Particle Swarm Optimization (BPSO) was employed for smart enhancement of UPFC performance in transmission systems and Artificial Neural Network Controller (ANNC) were also proposed by Rabab *et al.* (2019). The two proposed optimization techniques implemented using MATLAB software were reported for effective control of the UPFC parameters while the controller attained optimal performance, leading to improved

voltage stability and minimized transmission losses under various generation variation and load conditions. X-raying the reviewed literature, voltage stability improvement using approach such as ANN controlled UPFC is still a research gap that needs to be thoroughly explored in power system.

METHODOLOGY

Load Flow Analysis

The power flow equations representing the active power P_i and reactive power Q_i, respectively at any bus i in-line with Figure 1 (Gupta, 2011) are shown (1) and (2)

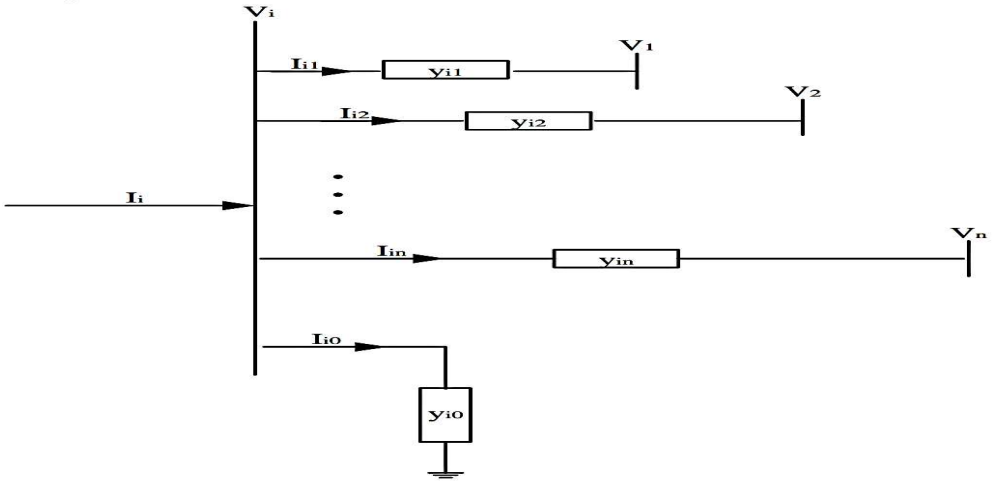

Figure 1: Typical Model of Power System (Gupta, 2011; Kothari and Nagrath, 2008).

$$P_i = |V_i| \sum_{k=1}^{n} |Y_{ik}||V_k| \cos(\theta_{ik} + \delta_k - \delta_i) \quad (1)$$

$$Q_i = -|V_i| \sum_{k=1}^{n} |Y_{ik}||V_k| \sin(\theta_{ik} + \delta_k - \delta_i) \quad (2)$$

$$i, k = 1, 2, \ldots . n$$

Where V_i is bus i voltage, V_k is bus k voltage, Y_{ik} is bus i to bus k transfer admittance, θ_{ik} is phase angular difference between buses i and k, δ_k is bus k phase angle, and δ_i is bus i phase angle.

Due to non-linearity of equations 1 and 2, numerical solution was provided by Newton-Raphson-based iterative technique leading to equation (3).

$$\begin{bmatrix} \Delta P_2 \\ \Delta P_3 \\ \vdots \\ \Delta P_n \\ \Delta Q_2 \\ \Delta Q_3 \\ \vdots \\ \Delta Q_n \end{bmatrix} = \begin{bmatrix} \frac{\partial P_2}{\partial \delta_2} & \frac{\partial P_2}{\partial \delta_3} & \cdots & \frac{\partial P_2}{\partial \delta_n} & \frac{\partial P_2}{\partial V_2} & \frac{\partial P_2}{\partial V_3} & \cdots & \frac{\partial P_2}{\partial V_n} \\ \frac{\partial P_3}{\partial \delta_2} & \frac{\partial P_3}{\partial \delta_3} & \cdots & \frac{\partial P_3}{\partial \delta_n} & \frac{\partial P_3}{\partial V_2} & \frac{\partial P_3}{\partial V_3} & \cdots & \frac{\partial P_3}{\partial V_n} \\ \vdots & \vdots & \vdots & \vdots & \vdots & \vdots & \vdots & \vdots \\ \frac{\partial P_n}{\partial \delta_2} & \frac{\partial P_n}{\partial \delta_3} & \cdots & \frac{\partial P_n}{\partial \delta_n} & \frac{\partial P_n}{\partial V_2} & \frac{\partial P_n}{\partial V_3} & \cdots & \frac{\partial P_n}{\partial V_n} \\ \frac{\partial Q_2}{\partial \delta_2} & \frac{\partial Q_2}{\partial \delta_3} & \cdots & \frac{\partial Q_2}{\partial \delta_n} & \frac{\partial Q_2}{\partial V_2} & \frac{\partial Q_2}{\partial V_3} & \cdots & \frac{\partial Q_2}{\partial V_n} \\ \frac{\partial Q_3}{\partial \delta_2} & \frac{\partial Q_3}{\partial \delta_3} & \cdots & \frac{\partial Q_3}{\partial \delta_n} & \frac{\partial Q_3}{\partial V_2} & \frac{\partial Q_3}{\partial V_3} & \cdots & \frac{\partial Q_3}{\partial V_n} \\ \vdots & \vdots & \vdots & \vdots & \vdots & \vdots & \vdots & \vdots \\ \frac{\partial Q_n}{\partial \delta_2} & \frac{\partial Q_n}{\partial \delta_3} & \cdots & \frac{\partial Q_n}{\partial \delta_n} & \frac{\partial Q_n}{\partial V_2} & \frac{\partial Q_n}{\partial V_3} & \cdots & \frac{\partial Q_n}{\partial V_n} \end{bmatrix} \begin{bmatrix} \Delta \delta_2 \\ \Delta \delta_3 \\ \vdots \\ \Delta \delta_n \\ \Delta V_2 \\ \Delta V_3 \\ \vdots \\ \Delta V_n \end{bmatrix} \quad (3)$$

Where ΔP is the real power change, ΔQ is the reactive power change, ΔV is the change in magnitude of bus voltage and $\Delta\delta$ is the deviation in phase angle of bus voltage.

The technique is versatile, accurate, reliable and converges faster (Gupta, 2011). Change in the reactive and real power at each iteration level with the new estimates of bus voltage magnitude and phase angle are given by equations (4) to (7):

$$\Delta P_i^r = P_i^{spec} - P_i^r \quad (4)$$

$$\Delta Q_i^r = Q_i^{spec} - Q_i^r \quad (5)$$

$$\delta_i^{r+1} = \delta_i^r + \Delta \delta_i^r \quad (6)$$

$$V_i^{r+1} = V_i^r + \Delta V_i^r \quad (7)$$

Where r is the iteration count, ΔP_i^r is the change in the real power at the iteration r, P_i^{spec} is the specified value of the real power, P_i^r is the calculated value of the real power at iteration r, ΔQ_i^r is the change in the reactive power at the iteration r,

Q_i^{spec} is the specified value of the reactive power, Q_i^r is the calculated value of the reactive power at the iteration r, δ_i^{r+1} is the new estimate of the bus voltage phase angle at the iteration $r+1$, δ_i^r is the calculated value of the bus voltage angle at the iteration r, $\Delta\delta_i^r$ is the change in the bus voltage phase angle at the iteration r, V_i^{r+1} is the new estimate of the bus voltage magnitude at the iteration $r+1$, V_i^r is the calculated value of the bus voltage magnitude at the iteration r, ΔV_i^r is the change in the bus voltage magnitude at the iteration r.

The specified reactive power and voltage constraints for effective performance of the system model in Figure 1 are given by equations (8) and (9), respectively:

$$V_{imin} \le V_i \le V_{imax} \quad (8)$$

$$Q_{imin} \le Q_i \le Q_{imax} \quad (9)$$

Where $V_{imin}$is the minimum voltage magnitude value at the bus *i*, V_{imax} is the maximum voltage magnitude value at the bus *i*, Q_{imin} is the minimum reactive power supply at the bus *i*, Q_{imax} is the maximum reactive power supply at the bus *i*.

Load Flow Model of UPFC

Figure 2 is the equivalent circuit model of the UPFC.

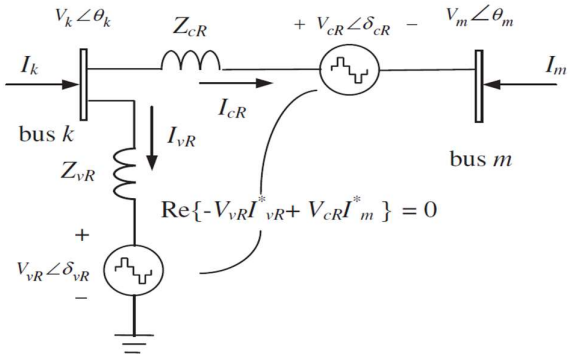

Figure 2: The UPFC equivalent circuit model (Acha *et al.*, 2004)

The voltage and power equations describing the operation of UPFC for power flow regulation between buses *k* and *m* are expressed by equations (10) to (12), respectively (Acha *et al*., 2004):

$$E_{VR} = V_{VR}(\cos\delta_{VR} + jsin\ \delta_{VR}) \quad (10)$$

$$E_{CR} = V_{CR}(\cos\delta_{CR} + jsin\ \delta_{CR}) \quad (11)$$

$$\begin{bmatrix} \Delta P_k \\ \Delta P_m \\ \Delta Q_k \\ \Delta Q_m \\ \Delta P_{mk} \\ \Delta Q_{mk} \\ \Delta P_{bb} \end{bmatrix} = \begin{bmatrix} \frac{\partial P_k}{\partial\theta_k} & \frac{\partial P_k}{\partial\theta_m} & \frac{\partial P_k}{\partial V_{vR}}V_{vR} & \frac{\partial P_k}{\partial V_m}V_m & \frac{\partial P_k}{\partial\delta_{cR}} & \frac{\partial P_k}{\partial V_{cR}}V_{cR} & \frac{\partial P_k}{\partial\delta_{vR}} \\ \frac{\partial P_m}{\partial\theta_k} & \frac{\partial P_m}{\partial\theta_m} & 0 & \frac{\partial P_m}{\partial V_m}V_m & \frac{\partial P_m}{\partial\delta_{cR}} & \frac{\partial P_m}{\partial V_{cR}}V_{cR} & 0 \\ \frac{\partial Q_k}{\partial\theta_k} & \frac{\partial Q_k}{\partial\theta_m} & \frac{\partial Q_k}{\partial V_{vR}}V_{vR} & \frac{\partial Q_k}{\partial V_m}V_m & \frac{\partial Q_k}{\partial\delta_{cR}} & \frac{\partial Q_k}{\partial V_{cR}}V_{cR} & \frac{\partial Q_k}{\partial\delta_{vR}} \\ \frac{\partial Q_m}{\partial\theta_k} & \frac{\partial Q_m}{\partial\theta_m} & 0 & \frac{\partial Q_m}{\partial V_m}V_m & \frac{\partial Q_m}{\partial\delta_{cR}} & \frac{\partial Q_m}{\partial V_{cR}}V_{cR} & 0 \\ \frac{\partial P_{mk}}{\partial\theta_k} & \frac{\partial P_{mk}}{\partial\theta_m} & 0 & \frac{\partial P_{mk}}{\partial V_m}V_m & \frac{\partial P_{mk}}{\partial\delta_{cR}} & \frac{\partial P_{mk}}{\partial V_{cR}}V_{cR} & 0 \\ \frac{\partial Q_{mk}}{\partial\theta_k} & \frac{\partial Q_{mk}}{\partial\theta_m} & 0 & \frac{\partial Q_{mk}}{\partial V_m}V_m & \frac{\partial Q_{mk}}{\partial\delta_{cR}} & \frac{\partial Q_{mk}}{\partial V_{cR}}V_{cR} & 0 \\ \frac{\partial P_{bb}}{\partial\theta_k} & \frac{\partial P_{bb}}{\partial\theta_m} & \frac{\partial P_{bb}}{\partial V_{vR}}V_{vR} & \frac{\partial P_{bb}}{\partial V_m}V_m & \frac{\partial P_{bb}}{\partial\delta_{cR}} & \frac{\partial P_{bb}}{\partial V_{cR}}V_{cR} & \frac{\partial P_{bb}}{\partial\delta_{vR}} \end{bmatrix} \begin{bmatrix} \Delta\theta_k \\ \Delta P_m \\ \frac{\Delta V_{vR}}{V_{vR}} \\ \frac{\Delta V_{vR}}{V_{vR}} \\ \partial\delta_{cR} \\ \frac{\Delta V_{cR}}{V_{cR}} \\ \partial\delta_{vR} \end{bmatrix} \quad (12)$$

where V_{VR} and δ_{VR} are the controllable voltage magnitude $\left(V_{VR,min} \le V_{VR} \le V_{VR,max}\right)$ and phase angle $(0 \le \delta_{VR} \le 2\pi)$ of the shunt converter (E_{VR}), V_{CR} and δ_{CR} are the controllable voltage magnitude $\left(V_{CR,min} \le V_{CR} \le V_{CR,max}\right)$ and the phase angle $(0 \le \delta_{CR} \le 2\pi)$ of the voltage source of series converter (E_{CR}), P_k and Q_k are the active and reactive power, respectively at the bus *k*, P_m and Q_m are the active and reactive power, respectively at the bus *m*, P_{CR} and Q_{CR} are the series converter's active and reactive power, respectively, P_{VR} and Q_{VR} are the shunt converter's active and reactive power, respectively.

Voltage Stability Index

Voltage Stability Index (VSI) is a metric that gives the measure of a network to transmit the power available without any negative consequence on the state of stability of the system. This metric was employed in this study because it provides useful details about the closeness of the power network to voltage instability. VSI is expressed mathematically as equation (13):

$$VSI = \frac{4Z_{ij}^2 Q_j}{u_i^j X_{ij}} \leq 1 \qquad (13)$$

ANN Controlled UPFC Architecture

Since FACTS generally involve high initial cost, their location, type and size are very essential and should be optimized to place them in power system networks for maximum efficiency. In this study, Artificial Neural Network (ANN) was adopted for optimal location of UPFC and the ANN controlled architecture employed is as shown in Figure 3.

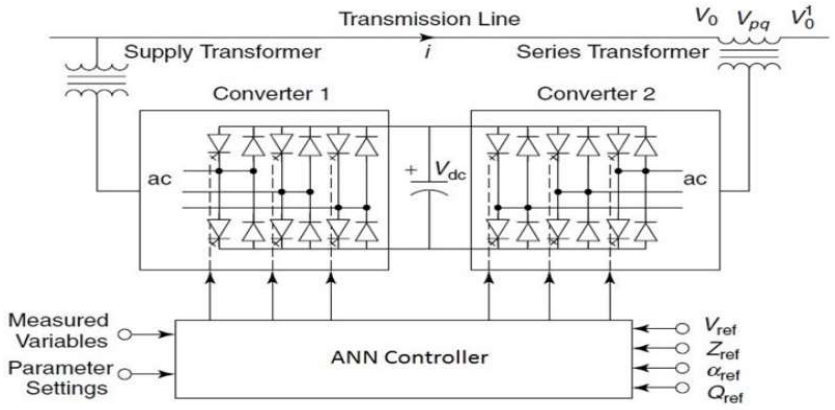

Figure 3: ANN Controlled Architecture for Optimal placement of UPFC in a Power System Network (Adapted from Mohanty and Viswavandy, 2015).

Implementation with MATLAB Neural Network Toolbox

The software tool employed to implement this study is MATLAB Neural Network toolbox.

It supports a collection of predefined neural network architectures and also enables researchers in analyzing processing of information in neural networks quickly (Paul, 2002).

Test Case

The Nigerian 330 kV, 30-Bus Power System

Figure 5 shows the one-line diagram of the Nigerian 330 kV, 30-bus power network that contains eleven generating stations, nineteen load buses and fifty-three transmission lines while Tables 1 and 2, respectively present the bus and line data.

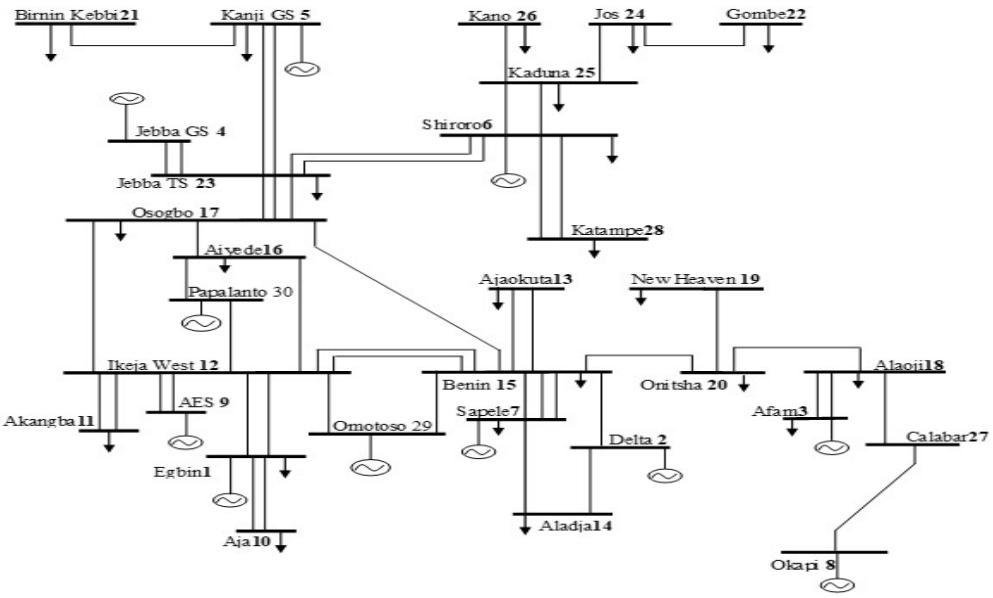

Figure 5: Nigerian 330 kV, 30-bus Power Network System

Table 1: Bus Data of the Nigerian 30-Bus Power Network

S/N	Bus Name	Bus Number	V	Angle	P_G	Q_G	P_D	Q_D
1	Egbin	1	1.05	0	0	0	68.9	51.7
2	Delta	2	1.05	0	670	0	0	0
3	Afam	3	1.05	0	431	0	52.5	39.4
4	Jebba GS	4	1.05	0	495	0	0	0
5	Kanji GS	5	1.05	0	624.7	0	7	5.2
6	Shiroro	6	1.05	0	388.9	0	70.3	36.1
7	Sapele	7	1.05	0	190.3	0	20.6	15.4
8	Okapi	8	1.05	0	750	0	0	0
9	AES	9	1.05	0	750	0	0	0
10	Aja	10	1	0	0	0	274.4	205.8
11	Akangba	11	1	0	0	0	344.7	258.5
12	Ikeja west	12	1	0	0	0	633.2	474.9
13	Ajaokuta	13	1	0	0	0	13.8	10.3
14	Aladja	14	1	0	0	0	96.5	72.4
15	Benin	15	1	0	0	0	383.3	287.5
16	Aiyede	16	1	0	0	0	275.8	206.8
17	Osogbo	17	1	0	0	0	201.2	150.9
18	Alaoji	18	1	0	0	0	427	320.2
19	New haven	19	1	0	0	0	177.9	133.4
20	Onitsha	20	1	0	0	0	184.6	138.4
21	BirninKebbi	21	1	0	0	0	114.5	85.9
22	Gombe	22	1	0	0	0	130.6	97.9
23	Jebba TS	23	1	0	0	0	11.3	8.2

S/N	Bus Name	Bus Number	V	Angle	P_G	Q_G	P_D	Q_D
24	Jos	24	1	0	0	0	70.3	52.7
25	Kaduna	25	1	0	0	0	193	144.7
26	Kano	26	1	0	0	0	220.6	142.9
27	Calabar	27	1	0	0	0	110	89
28	Katampe	28	1	0	0	0	290.1	145
29	Omotoso	29	1.05	0	410	0	0	0
30	Papalanto	30	1.05	0	342.10	0	0	0

Table 2: Line data Nigerian 30-bus power network

From Bus	To Bus	R (p.u)	X (p.u)	B (p.u)
Aja 10	Egbin 1	0.0006	0.0044	0.0295
Aja 10	Egbin 1	0.0006	0.0044	0.0295
Akangba 11	Ikeja west 12	0.0007	0.005	0.0333
Akangba 11	Ikeja west 12	0.0007	0.005	0.0333
Egbin 1	Ikeja west 12	0.0023	0.0176	0.1176
Egbin 1	Ikeja west 12	0.0023	0.0176	0.1176
Ikeja west 12	Benin 15	0.011	0.0828	0.55
Ikeja west 12	Benin 15	0.011	0.0828	0.55
Ikeja west 12	Aiyede 16	0.0054	0.0405	0.2669
Ikeja west 12	Osogbo 17	0.0099	0.0745	0.4949
Ajaokuta 13	Benin 15	0.0077	0.0576	0.383
Ajaokuta 13	Benin 15	0.0077	0.0576	0.383
Delta 2	Benin 15	0.0043	0.0317	0.2101
Delta 2	Aladja 14	0.0012	0.0089	0.0589
Aladja 14	Sapele 7	0.0025	0.0186	0.1237
Benin 15	Onitsha 20	0.0054	0.0405	0.2691
Benin 15	Osogbo 17	0.0098	0.0742	0.493
Benin 15	Sapele 7	0.002	0.0148	0.0982
Benin 15	Sapele 7	0.002	0.0148	0.0982
Benin 15	Sapele 7	0.002	0.0148	0.0982
Aiyede 16	Osogbo 17	0.0045	0.034	0.2257
BirninKebbi 21	Kanji GS 5	0.0122	0.0916	0.6098
Osogbo 17	Jebba TS 23	0.0061	0.0461	0.3064
Osogbo 17	Jebba TS 23	0.0061	0.0461	0.3064
Osogbo 17	Jebba TS 23	0.0061	0.0461	0.3064
Afam 3	Alaoji 18	0.001	0.0074	0.0491
Afam 3	Alaoji 18	0.001	0.0074	0.0491
Alaoji 18	Onitsha 20	0.006	0.0455	0.3045
New heaven 19	Onitsha 20	0.0036	0.0272	0.1807

From Bus	To Bus	R (p.u)	X (p.u)	B (p.u)
Gombe 22	Jos 24	0.0118	0.0887	0.5892
Jebba TS 23	Jebba GS 4	0.0002	0.002	0.0098
Jebba TS 23	Jebba GS 4	0.0002	0.002	0.0098
Jebba TS 23	Shiroro 6	0.0096	0.0721	0.4793
Jebba TS 23	Shiroro 6	0.0096	0.0721	0.4793
Jebba TS 23	Kanji GS 5	0.0032	0.0239	0.1589
Jebba TS 23	Kanji GS 5	0.0032	0.0239	0.1589
Jos 24	Kaduna 25	0.0081	0.0609	0.4046
Kaduna 25	Kano 26	0.009	0.068	0.4516
Kaduna 25	Shiroro 6	0.0038	0.0284	0.1886
Kaduna 25	Shiroro 6	0.0038	0.0284	0.1886
Shiroro 6	Katampe 28	0.0038	0.0284	0.1886
Shiroro 6	Katampe 28	0.0038	0.0284	0.1886
Alaoji 18	Calabar 27	0.0071	0.0532	0.38
Calabar 27	Okapi 8	0.0079	0.0591	0.39
Ikeja west 12	AES 9	0.0061	0.0118	0.0932
Ikeja west 12	AES 9	0.0061	0.0118	0.0932
Omotoso 29	Benin12	0.0024	0.0177	0.0325
Omotoso 29	Ikeja-West	0.00314	0.0236	0.0324
Papalanto 29	Ikeja-West	0.0032	0.0242	0.0475
1Papalanto 30	Aiyede 16	0.0038	0.0284	0.0475

RESULTS AND DISCUSSION

Results of load flow analysis on the Nigerian 30-bus system revealed six buses violated the statutory limit of $0.95 \leq V_i \leq 1.05$ p.u., namely: New Haven, Onitsha, Gombe, Jos, Kano and Calabar with voltage magnitude of 0.9003, 0.9468, 0.6608, 0.8141, 0.8138 and 0.9319 p.u., respectively, this occurred when no compensation was applied on the Nigerian 30-bus system and the system's total active power loss was 218.76 MW.

The simulation results of network's voltage profile, total active losses with and without compensation were compared using bar charts as presented in Figures 6 and 7, respectively.

Figure 6 revealed there were six critical buses in the Nigerian 330 kV, 30-bus power system whose voltage magnitudes fell out of the acceptable voltage tolerance limit of $0.95 \leq V_i \leq 1.05$ p.u. the buses are New Haven (19), Onitsha (20), Gombe (22), Jos (24), Kano (26) and Calabar (27) with their respective voltage magnitudes of 0.9003, 0.9468, 0.6608, 0.8141, 0.8138 and 0.9319 p.u. From these six constrained buses, Gombe with voltage magnitude of 0.6608 p.u. is the weakest followed by Kano, Jos, New Haven, Calabar and Onitsha. Also, from Figure 7, total active power loss in the network was 218.76 MW with no compensation device.

Using UPFC of five different sizes of 500, 600, 700, 800 and 1000 MVArs to manually but sequentially place them on each of the six constrained buses, starting with the Gombe bus (19) since it is the most critical bus within the network. The results obtained revealed that UPFC of 600 MVAr size had the most significant impacts on the active and reactive losses

of the all constrained buses. Moreso, the placement of UPFC at the bus Calabar (27) yielded the least total active power loss of 200.85 MW which is less than 218.76 MW (8.19% reduction) obtained when there was no compensation device. Four buses namely, New Haven (19), Gombe (22), Jos (24) and Kano (26) whose voltage magnitudes were 0.9130, 0.6608, 0.8141 and 0.8138 p.u., respectively, still violated the desired voltage tolerance limit.

With the application of ANN to optimally place UPFC, the VSI was computed and it was discovered that bus 22 (Gombe) would give the optimal location to place the UPFC on the network. The results as shown in Figure 6 revealed that apart from the voltage profile of overall network being enhanced, the voltage magnitudes of the six constrained Buses New Haven, Onitsha, Gombe, Jos, Kano and Calabar were improved to 0.9533, 0.9552, 1.0481, 1.0399, 1.0425 and 1.0081 p.u., respectively when compensated. Also, the system's total active power loss was reduced to 155.74 MW as presented in Figure 7 producing a significant reduction of 28.81%.

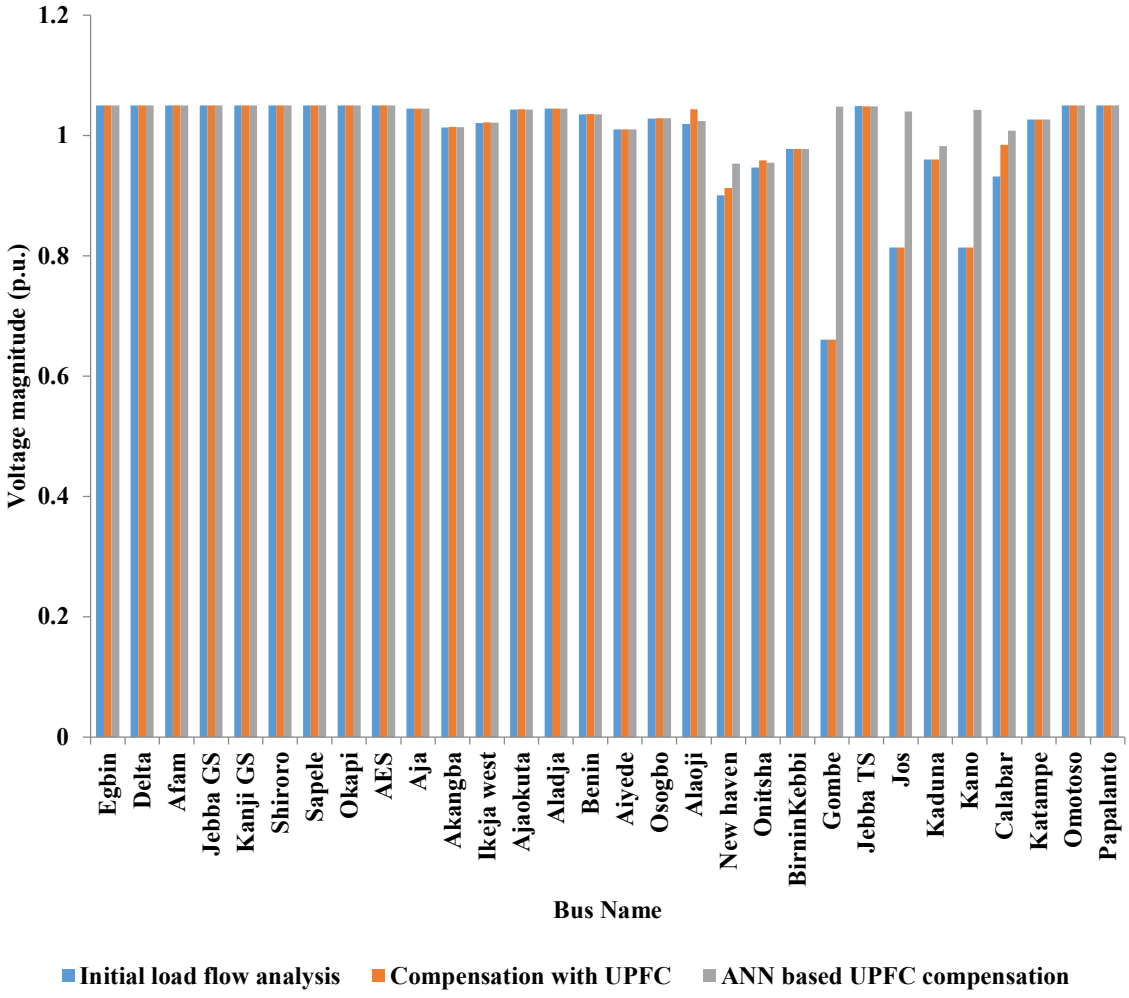

Figure 6: Comparison of the obtained voltage profile of the Nigerian 30-bus power network with and without compensation.

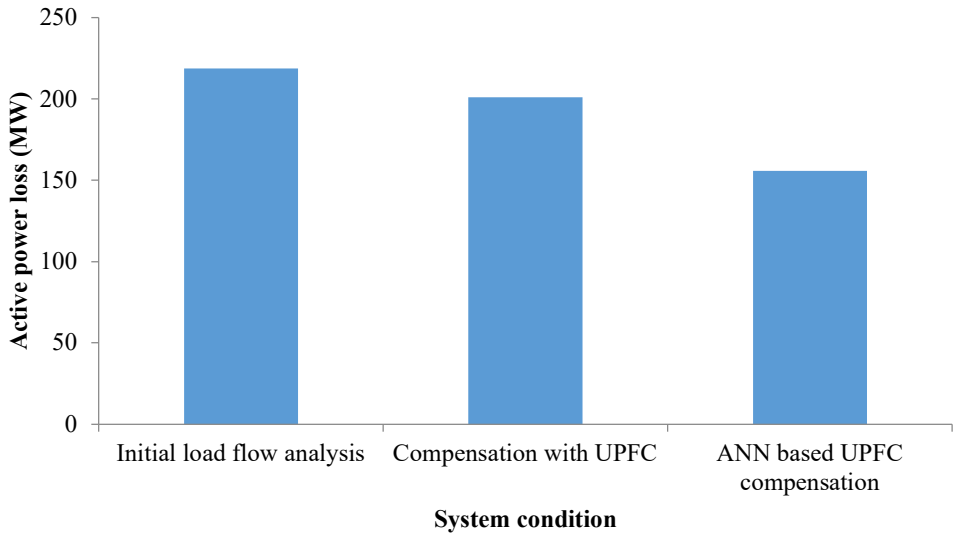

Figure 7: Comparison of the total active power loss on the Nigerian 30–bus power network with and without compensation.

CONCLUSION

This study considered an ANN based technique for optimal placement of UPFC for power system voltage stability improvement using the Nigerian 330 kV, 30-bus electricity grids as test network. Manual UPFC compensation on the Nigerian 30-bus power system although showed a good result in enhancing the total active power losses of the network but had a negligible impact on the voltage profile improvement because the voltage magnitudes of some buses were still constrained. ANN based UPFC compensation, however, did appreciably improved the voltage profile of the Nigerian 30–bus grid system with all buses of the system now within the acceptable voltage tolerance limit. Equally, the total active power loss of the system was also appreciably minimized with ANN based UPFC compensation. Therefore, as revealed in this study, the ANN controlled UPFC compensation employed is a suitable approach that could be deployed to enhance power system voltage stability and reduce power loss on power system, in order to have more spares of electrical energy that could be used to meet the need of consumers.

REFERENCES

Acha, E., Fuerte-Esquivel, C.R., Ambriz-Pe'rez, H., Angeles-Camacho, C. (2004). FACTS: Modelling and Simulation in Power Networks. John Wiley and Sons Limited, West Sussex, England.

Alhassan F., Abubakar A. S., Yusuf, J., Yusuf S., Idris K. (2020). Enhancement of Voltage Stability using Generalized Unified Power Flow Controller. Journal of Science Technology and Education, 8(2):189 – 198.

Chappa, H. and Thakur, T. (2020). Voltage Instability Detection Using Synchronous Measurements: A Review. International Transactions on Electrical Energy Systems, 30(6): e12343.

Ezeruigbo E. N., Ekwue A. O., Anih L. U. (2021). Voltage Stability Analysis of Nigerian 330kV Power Grid using Static P-V Plots. Nigerian Journal of Technology, Vol. 40, No. 1, January, 2021, pp. 70–80.

Gupta, B.R. (2011). Power System Analysis and Design. S. Chand and Company Ltd, New Delhi, India.

Gupta, M., Joshi, H., Gupta, A.K. and Sharma, N.K. (2022). A Review on Various Application of Several FACTS Controllers. International Journal of Advanced Research and Innovative Ideas in Education, 8(5): 130 – 143.

Idris, A.A., Abel, E.A. (2021). Enhancement of Voltage Stability in an Interconnected Network using unified power flow controller. Journal of Advances in Science and Engineering, 4:65 – 74.

Kumar, B.V. (2019). Optimal Location of UPFC to Improve Power System Voltage Stability Using Artificial Bee Colony Algorithm. American Journal of Electrical Power and Energy Systems, 8(2): 42 – 49.

Mohanty, A. and Viswavandy, M. (2015). A Novel ANN based UPFC for Voltage Stability and Reactive Power Management in a Remote Hybrid System. Science direct Procedia Computer Science, 48:555 – 560.

Muhammad, N., Kashif, I., Abraiz, K., Absin, U., Anamitra, P., Muhammad, Z. Z., Atif, N. K. and Malhar, P. (2020). Optimal placement, sizing and coordination of FACTS devices in transmission network using whole optimization algorithm, Energies13(3):753.

Mutegi, A.M., Muriithi, C.M. and Saulo, M.J. (2015). A review on voltage stability using artificial neural network controlled FACTS devices. Proceedings of the 2016 Annual Conference on Sustainable Research and Innovation, 138-143.

Noor, W., Musa, S., Rebaz, J. A. and Rusli, H. (2013). Optimization Techniques for Location of Flexible AC Transmission System Devices in Power Systems. Journal of Engineering Science and Technology Review, 6(5):61 – 66.

Paul, S. (2002). Neural Networks in Encyclopedia of the Human Brain. (Online). Available at https://www.sciencedirect.com/topics/neuroscience/neural-networks(13 August, 2020).

Patel, K. M., Khatua, K. and Yadav, N. (2014). Optimal placement of UPFC to enhance power system voltage stability. International Journal of Engineering Development and Research, 2 (RTEECE Conference): 49 – 52.

Rabab, R.M.E., Ebrahim A.B. and Ibrahim I.I.M. (2019). Smart Enhancement of UPFC Performance in Transmission Systems Using BPSO and ANNC. European Journal of Electrical and Computer Engineering, 3(5):1 – 8.

Rajesh, C. (2018). Artificial intelligence: An Approach in Power Systems. (Online). Available at https://www.electricalindia.in/artificial-intelligence-an-advanced-approach-in-power-systems/.Accessed 11 August, 2021